

Photodisintegration of ${}^3\text{He}$ in the Peak Region

S. Naito,^a K. Tamura,^a Y. Nagai,^a T. Shima^a and H. Toyokawa^b

^a*Research Center for Nuclear Physics, Osaka University, 10-1, Mihogaoka, Ibaraki, Osaka
567-0047, Japan*

^b*Quantum Radiation Division, Electrotechnical Laboratory (ETL), Tsukuba, Ibaraki
305-8568, Japan*

The nuclear reactions of the three-nucleon system, i.e. ${}^3\text{H}$ and ${}^3\text{He}$, provide unique tools for investigations of the three-body problem and the nucleon-nucleon (NN) interactions including the 3N force. In the last decades there have been a big advance in theoretical methods for treating three-body system, and the theoretical calculations for the photodisintegration cross sections of ${}^3\text{He}$ and ${}^3\text{H}$ have been carried out with the use of those methods[1-7]. According to the results of those calculations, it has been pointed out that the photodisintegration cross sections in the peak energy region ($E_\gamma = 10\sim 20\text{MeV}$) are sensitive to the NN potential. For example, Schadow et al. predicted the ${}^3\text{He}(\gamma, p)d$ cross section at $E_\gamma \sim 10\text{MeV}$ varies by $\sim 20\%$ depending on the choice of the NN potential[7]. And Efros et al. pointed out the maximum of the ${}^3\text{He}$ total photoabsorption cross section is reduced by $\sim 10\%$ if the 3N forces like the Urbana-VIII or Tucson-Melbourne potentials are incorporated[6]. Therefore it is quite important to determine experimentally the cross sections in the peak region. However, the existing experimental data for those reaction cross sections are much inconsistent with each other, and that is quite unsatisfactory for the above studies. For that reason we made a new precise measurement of the photodisintegration cross sections of ${}^3\text{He}$ in the peak region using a new experimental method as shown below.

In order to determine the accurate cross sections, we used the time projection chamber (TPC)[8] and Laser Compton-Scattered (LCS) γ beam at Electrotechnical Laboratory (ETL)[9]. Since the TPC contains an active gas target made of ${}^3\text{He}$ (640Torr) together with the quenching gas of methane (160Torr), charged particles from the photodisintegration of ${}^3\text{He}$ can be detected with almost 100% detection efficiency and 4π acceptance. TPC detects the tracks of the charged particles from the reactions, and that enables us to distinguish precisely the reaction events of ${}^3\text{He}(\gamma, p)d$, ${}^3\text{He}(\gamma, pp)n$, and the other backgrounds. Furthermore, since the LCS γ beam is quasi-monochromatic and well-collimated, the background events can be rejected efficiently. The above characteristic features of the present method are advantages for precise measurement of the cross sections. The measurement was carried out at the γ -ray energies of 10.5MeV and 16.5MeV.

Figures 1 and Figure 2 show the obtained cross sections for ${}^3\text{He}(\gamma, p)d$ and the total photoabsorption, respectively. Thanks to the advantages of the present method, the systematic error of the measurement was less than 3%. The present results are consistent with the smaller values of the cross sections from the previous experiments for ${}^3\text{He}(\gamma, p)d$ [12][16] and total photoabsorption[19], and smaller than the theoretical calculations by $\sim 15\%$. Therefore it is important to study further the choice of the NN potentials, the effects of the E1-E2 interference and the contribution of the meson-exchange currents.

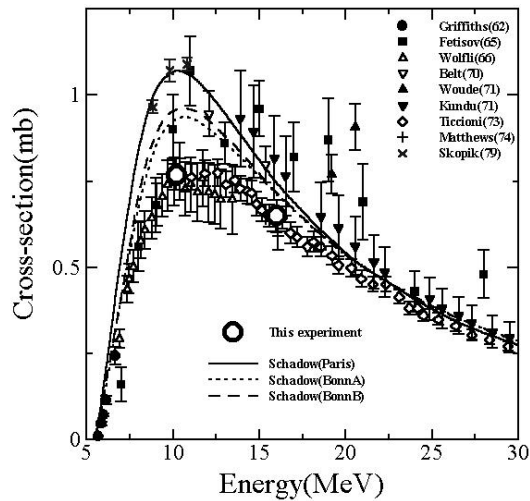


Figure 1: Excitation function of ${}^3\text{He}(\gamma,p)d$. Circle; present, closed circle; Ref.10, closed square; Ref.11, open triangle; Ref.12, open rev. triangle; Ref.13, closed triangle; Ref.14, closed rev. triangle; Ref.15, diamond; Ref.16, cross; Ref.17, diag. cross; Ref.18. The solid, dotted and dashed lines are the calculations from Ref.7.

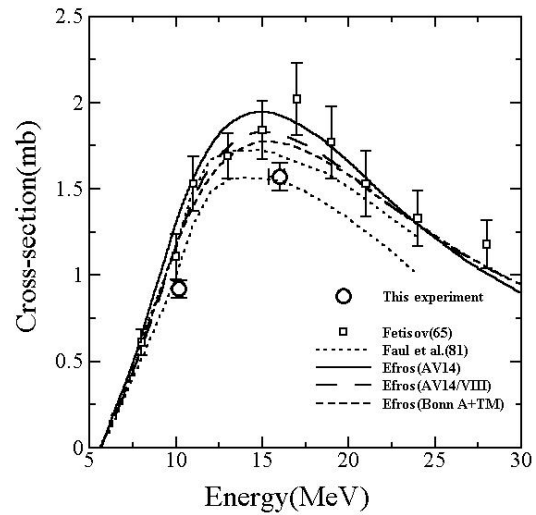


Figure 2: Excitation function of total photoabsorption. Circle; present, open square; Ref.11. The dotted curves are the upper and lower limits of the experimental cross sections given by Faul et al.[19]. The solid, long-dashed and short-dashed curves are the calculations by Efros et al. with the NN potentials of AV14, AV14+UrbanaVIII and BonnA+TM, respectively[6].

References

- [1] W. Sandhas et al., Nucl. Phys. **A631** (1998) 210c.
- [2] W. Schadow and W. Sandhas, Phys. Lett. **55C** (1997) 1074.
- [3] W. Schadow and W. Sandhas, Nucl. Phys. **A631** (1998) 588c.
- [4] V.D. Efros, W. Leidemann and G. Orlandini, Phys. Lett. **408B** (1997) 1.
- [5] V.D. Efros, W. Leidemann and G. Orlandini, Nucl. Phys. **A631** (1998) 658c.
- [6] V.D. Efros et al., Phys. Lett. **484B** (2000) 223.
- [7] W. Schadow, O. Nohodani and W. Sandhas, Phys. Rev. **C63** (2001) 044006.
- [8] T. Shima et al, Nucl. Phys. **A687** (2001) 127c.
- [9] H. Ohgaki et al., IEEE Trans. Nucl. Sci. **38** (1991) 386.
- [10] G.M. Griffiths, E.A. Larson and L.P. Robertson, Can. J. Phys. **40** (1962) 402.
- [11] V.N. Fetisov, A.N. Gorbunov and A.T. Varfolomeev, Nucl. Phys. **71** (1965) 305.
- [12] W. Wolfli et al., Phys. Lett. **22** (1966) 75.
- [13] B.D. Belt et al., Phys. Rev. Lett. **24** (1970) 20.
- [14] A. van der Woude et al., Phys. Rev. Lett. **26** (1971) 909.
- [15] S.K. Kundu, Y.M. Shin and G.D. Wait, Nucl. Phys. **A171** (1971) 384.
- [16] G. Ticcioni, S.N. Gardner, J.L. Matthews and R.O. Owens, Phys. Lett. **46B** (1973) 369.
- [17] J.L. Matthews et al., Nucl. Phys. **A223** (1974) 221.
- [18] D.M. Skopik et al., Phys. Rev. **C19** (1979) 601.
- [19] D.D. Faul, B.L. Berman, P. Meyer and D.L. Olson, Phys. Rev. **C24** (1981) 849.